ACS OMEGA

http://pubs.acs.org/journal/acsodf

Article

Magnetite Nanoparticles Functionalized with Thermoresponsive Polymers as a Palladium Support for Olefin and Nitroarene Hydrogenation

Sujittra Paenkaew, Usana Mahanitipong, Metha Rutnakornpituk,* and Oliver Reiser*

Cite This: *ACS Omega* 2023, 8, 14531−14540

Read Online

ACCESS | Metrics & More | Article Recommendations | Supporting Information

ABSTRACT: A thermoresponsive and recyclable nanomaterial was synthesized by surface modification of magnetite nanoparticles (MNPs) with poly(*N*-isopropylacrylamide-*co*-diethylaminoethyl methacrylate) (P(NIPAAm-*co*-DEAEMA)), having PNIPAAm as a thermoresponsive moiety and PDEAEMA for catalyst binding. Palladium (Pd) nanoparticles were incorporated into this material, and the resulting nanocatalyst was efficient in the hydrogenation of olefins and nitro compounds with turnover frequencies (TOFs) up to 750 h^{-1}. Consistent catalytic activity in 10 consecutive runs was observed when performing the hydrogenation at 45 °C, i.e., above the lower critical solution temperature (LCST) of the copolymer (37 °C), followed by cooling to 15 °C, i.e., below the LCST of the copolymer.

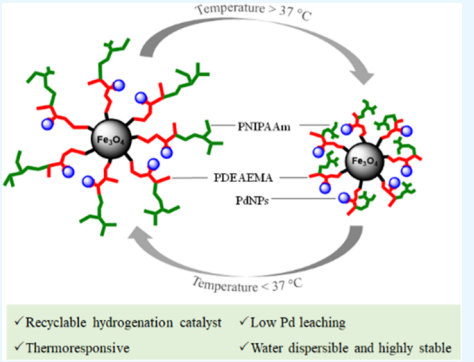

INTRODUCTION

Nowadays, highly active and selective metal catalysts for hydrogenation play an essential role in chemical industries by advocating both their economic success and environmental sustainability.[1] Important classes of substrates for this technology are alkenes and nitroarenes, which are recognized to be of great synthetic value.[2,3] Arguably, the most active hydrogenation catalysts are based on palladium,[4] rhodium,[5] and iridium;[6] however, costly noble metals and ligands are often irrecoverable after completing reactions, and moreover, even trace amounts of metal species need to be removed from a product to meet the stringent requirements, especially for pharmaceutical chemistry.[7] During the past decade, reusable catalysts have been of increasing interest because they can overcome these problems.[8,9] Heterogenization is the key strategy to achieve recoverable systems, which can be retrieved *via* various recovering strategies such as filtration[10−12] or centrifugation and magnetic separation.[13,14]

Magnetite nanoparticles (MNPs) have emerged as excellent solid supports owing to their good magnetic response and high oxidation stability, allowing various applications in many areas such as the biomedical, pharmaceutical, and chemical fields.[15] They are particularly studied as catalyst supports owing to their high surface-area-to-volume ratio, which makes them attractive for the immobilization of noble metal catalysts.[16−20] However, MNPs tended to aggregate due to dipole−dipole, gravity, and magnetic attractive forces, leading to the loss of their nanoscale-related properties.[21−23] Polymeric coating of MNPs is therefore a promising approach to improve their dispersibility in the media due to charged repulsion and/or steric repulsion of polymer chains.[24−26] Moreover, polymer coating also allows the introduction of a wide spectrum of functional groups, which can be used to improve the incorporation of catalysts onto the magnetic support.[27−29]

Stimuli-responsive polymers are useful for a wide range of various applications because their properties can be altered to respond to environmental impulses, such as temperature, pH, light, electrostatic, electrical, magnetic field, etc.[30−33] A number of reports have described the immobilization of catalysts into stimuli-responsive polymers to date. For example, Dong et al. have designed stimuli-sensitive poly(acrylamide-*co*-acrylic acid)-stabilized Pd nanoparticles that can change their conformation in response to pH and temperature variations to allow good recyclability and high catalytic activity in hydrogenations of phenol and allyl alcohol in aqueous media.[34] Li et al. presented the grafting of thermoresponsive poly[(*N*-isopropylacrylamide)-*co*-(glycidyl methacrylate)] (P(NIPAAm-*co*-GMA)) onto nanocellulose sponges, which served as a support for gold nanoparticles.[35] Again, good catalytic activity and recyclability for 22 cycles in the reduction of 4-nitrophenol were demonstrated. In addition, there are many other reports involving the use of stimuli-responsive

Received: January 7, 2023
Accepted: March 13, 2023
Published: April 12, 2023

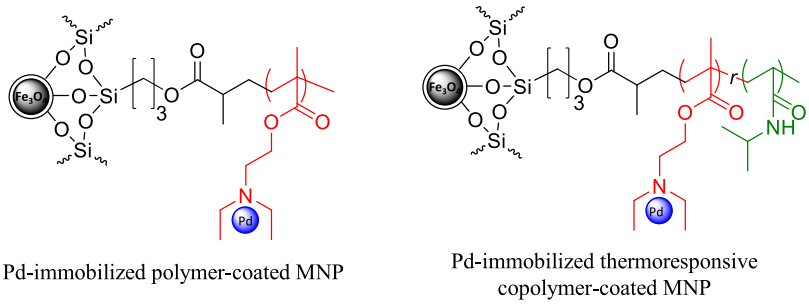

Figure 1. Pd-immobilized polymer-coated MNPs used in this work.

polymers as supports of other catalyst systems, e.g., for Ru,[36] Ni,[37] Ag,[38] and Zn.[39]

PNIPAAm is one of the most interesting thermoresponsive polymers owing to its sharp change of physicochemical behaviors with the temperature below and above the lower critical solution temperature (LCST of PNIPAAm ≈ 32 °C).[40] At the temperature below its LCST, the polymer chains undergo swelling (hydrophilic behavior) due to the formation of intermolecular hydrogen bonds between amide groups of PNIPAAm chains and water molecules.[41] This can produce swollen carriers on the surface of materials, which improve the retention of catalyst and thus assist in the catalyst stability in aqueous media. At the temperature above its LCST, PNIPAAm chains display shrinkage behavior (hydrophobic state) due to intramolecular hydrogen bonds among amide groups,[42] allowing facile access of starting materials to catalysts being stabilized on the surface of the thermoresponsive support. Hence, with a rational design of the polymer structure coating on the support, the exploitation of these attractive properties can lead to a new kind of thermoresponsive catalytic system.[43,44]

We report here the synthesis of thermo- and magnetic-responsive nanosupports for the immobilization of transition-metal nanoparticles and their application in catalytic hydrogenation reactions. Poly(diethylaminoethyl methacrylate) (PDEAEMA) homopolymer and poly(*N*-isopropylacrylamide-*co*-diethylaminoethyl methacrylate) (P(NIPAAm-*co*-DEAEMA)) copolymers were coated onto MNPs to serve as a platform having amino groups of DEAEMA units for coordinating noble metal-based nanoparticles and PNIPAAm as thermoresponsive moieties (Figure 1). Pd was used as a representative agent because it is typically used in hydrogenations employed in many chemical and pharmaceutical industries.[45−48] Substituting conventional homogeneous reduction systems with heterogeneous catalysts to allow efficient recovery of scarce metals by magnetic separation is the motivation of this study. The characteristic properties of the material developed, such as particle distribution, hydrodynamic size, magnetic properties, and catalytic activity, were investigated. Especially relevant, the effect of temperature variation on catalytic performance and recycling ability was evaluated.

EXPERIMENTAL SECTION

Synthesis of Methacrylate-Coated MNPs as a Cross-linker 3. MNPs were synthesized *via* a coprecipitation method in an aqueous solution. $FeCl_3$ (1.66 g, 10.2 mmol in 20 mL of deionized water) and $FeCl_2{\cdot}4H_2O$ (1.00 g, 5.1 mmol in 20 mL of deionized water) were mixed together. Then, NH_4OH (20 mL) was added dropwise into the solution to obtain a black precipitant and kept stirring for 30 min to complete the reaction. The MNP **1** was magnetically separated and washed with deionized water (3×) and then toluene (3×). After slow addition of oleic acid (2 mL) into the MNP dispersion (0.5 g in 20 mL of toluene) for 30 min to obtain **2**, 3-(trimethoxysilyl)propyl methacrylate (TMSPMA) (5.15 mL, 10 equiv) and triethylamine (TEA) (0.5 mL) were introduced with vigorous stirring for 24 h under a N_2 atmosphere. The resulting methacrylate-coated MNP **3** was precipitated with the help of an external magnet, washed with hexanes (3×), and finally dried *in vacuo*. Elemental microanalysis (%): 8.31 C; 1.59 H; 0 N.

Preparation of PDEAEMA-Coated MNP (4a) and P(NIPAAm-*co*-DEAEMA)-Coated MNP (4b). P(NIPAAm-*co*-DEAEMA)-coated MNP **4b** was synthesized via free radical polymerization. NIPAAm (155 mg, 1.37 mmol), DEAEMA (254 mg, 1.37 mmol), and 2,2′-azobis(2-methylpropionitrile) (AIBN) as an initiator (4.5 mg, 0.0274 mmol) were added into the dispersion of methacrylate-coated MNP **3** (50 mg) in anhydrous 1,4-dioxane (2.7 mL) for 6 h at 70 °C under a nitrogen atmosphere. After the reaction was completed, the polymerization was ceased by cooling to room temperature. The product was separated using a permanent magnet and washed with 1,4-dioxane (2 × 5 mL) and then methanol (2 × 5 mL). Finally, the product was dried *in vacuo*. Elemental microanalysis (%): 17.47 C; 2.97 H; 1.17 N. PDEAEMA-coated MNP **4a** was synthesized using the same polymerized condition as described above with the use of solely DEAEMA (500 mg, 2.70 mmol) in the system. Elemental microanalysis (%): 16.02 C; 2.75 H; 1.28 N.

Synthesis of Pd-Immobilized Magnetic PDEAEMA (5a) and P(NIPAAm-*co*-DEAEMA) Composites (5b). The procedure for the synthesis of the catalysts using a 1:0.1 mass ratio of **4a**/**4b** to Pd is described herein. After sonicating for 10 min, to a dispersion of **4a** or **4b** (50 mg in 2 mL of Millipore water) was added 1 M HCl to adjust the mixture to pH 6, followed by the dropwise addition of $PdCl_2$ (8.33 mg, 47.02 μmol in 5 mL of Millipore water). $NaBH_4$ (17.8 mg in 1 mL of water) was introduced into the dispersion with vigorous stirring for 30 min. The resulting materials **5a** or **5b** were separated from the dispersion using a magnet, washed with water (5 × 10 mL), and dried *in vacuo*. **5a** contained (ICP-OES) 4.01 mg of Pd and 0.75 mmol of Pd/g (80.3% Pd incorporation). **5b** contained (ICP-OES) 4.07 mg of Pd and 0.77 mmol of Pd/g (81.4% Pd incorporation).

General Procedure for Hydrogenation Using Pd-Immobilized Magnetic PDEAEMA (5a) and P(NIPAAm-*co*-DEAEMA) Composites (5b) as Catalysts. To a Schlenk flask, **5a** (13.3 mg) or **5b** (13.0 mg) in 10 mL of isopropanol was sonicated for 10 min. Substrates (olefins or nitroarene (1

https://doi.org/10.1021/acsomega.3c00117
ACS Omega 2023, 8, 14531−14540

Scheme 1. Synthesis of Pd Catalyst (Blue Balls) Immobilized on P(NIPAAm-*co*-DEAEMA)-Coated MNP (Gray Balls) 5b and PDEAEMA-Coated MNP 5a

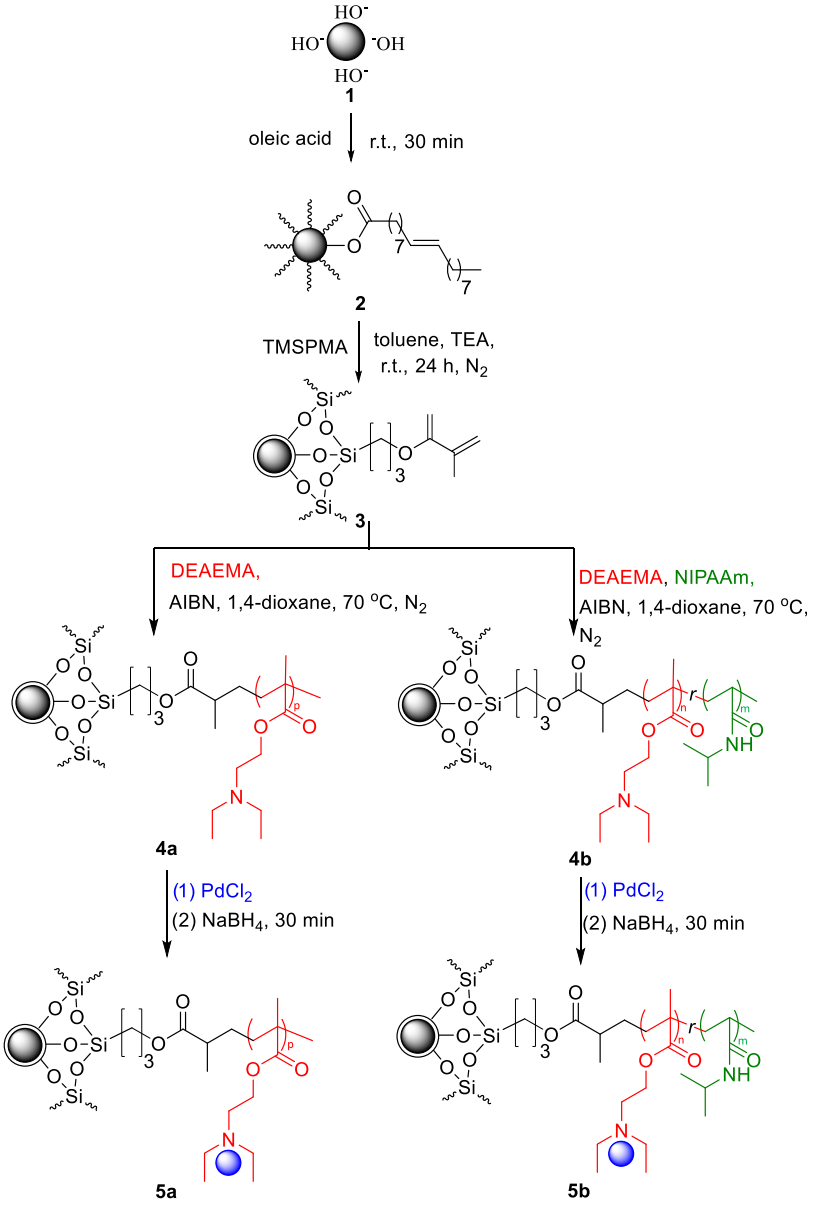

mmol)) and dodecane (77.6 μL, 58.17 mg, 0.5 mmol) as an internal standard were added and the mixture was stirred under 1 atm H_2-pressure (balloon) at 25 °C for the indicated time (the reaction progress was monitored by gas chromatography (GC) analysis). Turnover frequency (TOF) values were calculated from the mole of the substrates transformed per mole of the catalyst (Pd) per hour (t)

$$\text{TOF} = (\text{mole of the substrates transformed/mole of Pd used})/t$$

Effect of Temperature on Catalytic Activity and Recycling Ability. Hydrogenation was studied with **5a** or **5b** using 4-chlorostyrene as a model substrate at 25 °C (T < LCST) and 45 °C (T > LCST). After sonicating the mixture of **5a** (13.3 mg) or **5b** (13.0 mg) in isopropanol (10 mL) for 10 min, 4-chlorostyrol (127 μL, 138.6 mg, 1 mmol) and dodecane (77.6 μL, 58.17 mg, 0.5 mmol) as an internal standard were added into the mixture with continuous stirring under 1 atm H_2-pressure (balloon). The dispersion was then purified by magnetic separation, washed with isopropanol (2 × 5 mL) and dichloromethane (2 × 5 mL), and dried *in vacuo* before using it for the next cycle.

RESULTS AND DISCUSSION

Superparamagnetic MNP **1** was selected as a magnetic support because of its high stability against oxidation and rapid response to a permanent magnet. First, methacrylate-coated MNP **3** was synthesized through the reaction between oleic-coated MNP **2** and TMSPMA (Scheme 1), followed by copolymerization with DEAEMA and NIPAAm monomers in the presence of AIBN as a radical initiator. The mass ratio of [methacrylate-coated MNP]/[monomers] was equal to 1:20, while the molar ratio of [AIBN]/[DEAEMA]/[NIPAAm] used in this step was 1:100:0 for PDEAEMA-coated MNP **4a** and 1:50:50 for P(NIPAAm-*co*-DEAEMA)-coated MNP **4b**.

https://doi.org/10.1021/acsomega.3c00117
ACS Omega 2023, 8, 14531−14540

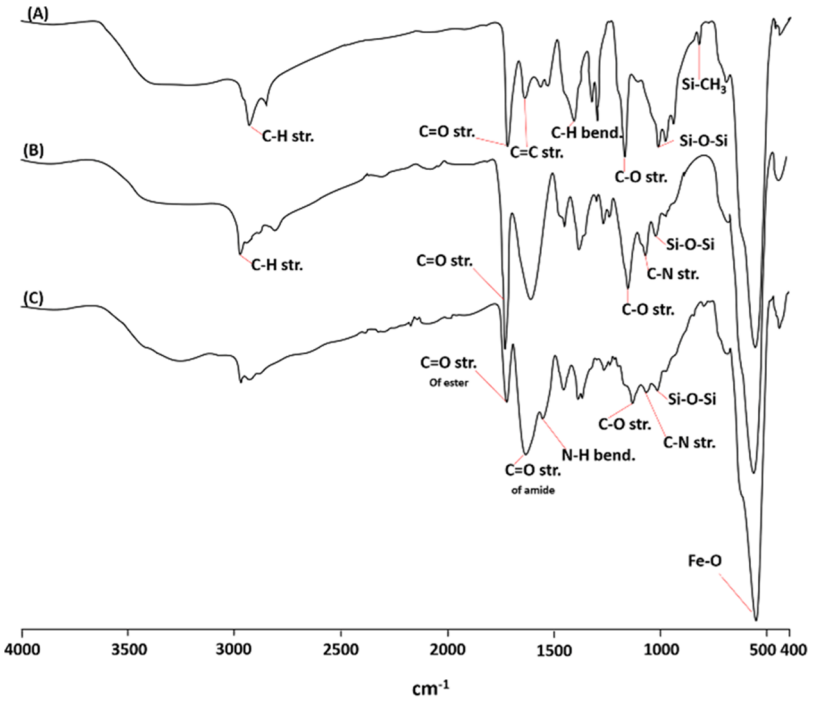

Figure 2. FTIR spectra of (A) methacrylate-coated MNP, (B) PDEAEMA-coated MNP, and (C) P(NIPAAm-co-DEAEMA)-coated MNP.

The feed molar ratio of NIPAAm/DEAEMA of 50:50 was selected in the copolymer synthesis because the presence of both several coordinating sites from PDEAEMA for Pd and sufficient PNIPAAm moieties to retain the thermoresponsive properties in the copolymer was desirable. Copolymers having a too low content of PNIPAAm resulted in the loss in the desirable thermoresponsive behavior, while those having too low PDEAEMA content led to a decrease in its coordination ability to Pd. It was found that both **4a** and **4b** were well dispersible and highly stable in the media (e.g., water, isopropanol, ethanol) and also easily recoverable by an external magnet within a few minutes.

FTIR spectra of methacrylate-coated MNP (the precursor) and PDEAEMA- and copolymer-coated MNP **4a** and **4b** revealed the successful grafting of the polymers onto **3** (Figure 2). The characteristic absorption peak of the iron oxide bond (Fe−O) at ca. 555 cm^{-1} is present in all compounds. PDEAEMA-coated MNP **4a** exhibited typical signals at 1019 cm^{-1} (silicone oxide, Si−O), 1065 cm^{-1} (C−N), 1149 cm^{-1} (C−O), 1727 cm^{-1} (C═O), and 2969 cm^{-1} (C−H), confirming the presence of PDEAEMA on the MNP surface (Figure 2B). Copolymer-coated MNP **4b** showed signals at 1013 cm^{-1} (silicone oxide, Si−O), 1064 cm^{-1} (C−N), 1129 cm^{-1} (C−O), 3263 and 1550 cm^{-1} (N−H), 1633 cm^{-1} (C═O, amide), 1719 cm^{-1} (C═O, ester), and 2969 cm^{-1} (C−H), signifying the presence of the copolymer on the surface of MNP **3** (Figure 2C).

Assuming that the *m*/*n* ratio of the copolymers grafted on the MNP surface resembled those of the ungrafted ones, the copolymer was synthesized using the same method described in the synthesis part without the addition of MNP **3** and used for structural analysis by ^{1}H NMR. Once the synthesis was completed, the polymer solution was dialyzed against methanol, refreshed three times, and dried *in vacuo*. From the ^{1}H NMR spectrum and the calculation shown in the Supporting Information (Figure S1), the *m*/*n* ratio in P(NIPAAm-*co*-DEAEMA) was about 9:6, indicating that the copolymer composition was about 60:40 molar ratio of NIPAAm to DEAEMA. The formation of the copolymer with a statistical distribution was confirmed by the presence of a single LCST at 37 °C, and this value was significantly different from its original LCST (32 °C). The presence of 60% of PNIPAAm as a majority in the copolymer chains resulted in preserving its thermoresponsive properties.

The LCST of **4b** was investigated by determining the change of its hydrodynamic diameter (D_h) as a function of temperature (Figure 3), which was increased stepwise in 5°

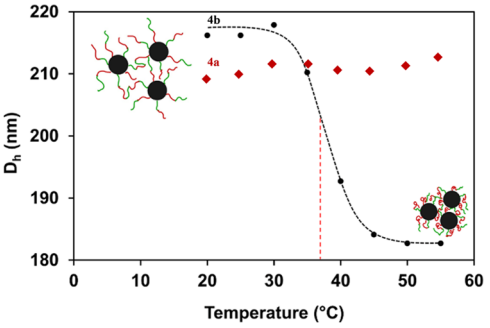

Figure 3. D_h changes of **4a** and **4b** as a function of temperature. The particle concentration in DI water was 200 ppm.

intervals from 20 to 55 °C with 2 min equilibrating time before data recording. The D_h of **4b** was steady at the temperature below 30 °C but showed a sharp decrease between 30 °C (D_h = 218 nm) and 45 °C (D_h = 184 nm) with only a slight change of D_h from this temperature onward. This is rationalized by the weakening of the hydrophilic interactions between water molecules and amide bonds and the strengthening of the hydrophobic interactions among amide bonds, resulting in the collapse of the copolymer on the MNP surface and thus decreasing D_h. The LCST transition value was about 37 °C

https://doi.org/10.1021/acsomega.3c00117
ACS Omega 2023, 8, 14531−14540

(Figure 3), which is higher than that of the PNIPAAm homopolymer (≈32 °C), being attributed to the presence of hydrophilic PDEAEMA moieties that affect the shrinkage of PNIPAAm in the copolymer.[49] The increase of the LCST due to the presence of hydrophilic polymers, especially PDEAEMA,[50] in the PNIPAAm-containing copolymer has been previously reported.[51−53] In the case of no PNIPAAm on the particles, the D_h of **4a** did not significantly change by increasing the temperature due to the absence of its thermoresponsive moiety. Notably, the changes of D_h of **5a** and **5b** showed similar trends compared to those of **4a** and **4b**.

Palladium nanoparticles were generated *in situ* by reduction of $PdCl_2$ with $NaBH_4$ in the presence of **4a** and **4b**, giving rise to Pd@PDEAEMA-coated MNP **5a** and Pd@P(DEAEMA-*co*-NIPAAm)-coated MNP **5b** (Table 1). The percentages of Pd incorporated were high (96−98% Pd for **5a** and 93−96% Pd for **5b**) when the mass ratio of **4a** or **4b** to Pd employed in the synthesis was up to 1:0.05 (entries 2, 3, 5, and 6). However, a further increase of Pd employed in the synthesis (entries 1 and 4) decreased the incorporation in the materials (80% Pd for **5a** and 81% Pd for **5b**), suggesting that the limit of the Pd uptake in the materials might be reached. Although the Pd incorporation in the latter cases (entries 1, 4) was comparatively lower, the high Pd content obtained in the resulting materials (8.03 wt % Pd for **5a** and 8.14 wt % Pd for **5b**) made these most promising for further evaluation. No significant effect of the NIPAAm moiety in the copolymer on the capability of Pd incorporation was observed, signifying that NIPAAm units do not hinder the coordinating capability of Pd for the amino groups of DEAEMA on the MNP surface.

Table 1. Syntheses of 5b and 5a Catalysts Having Various Pd Loadings

entries	catalysts	mass ratio[a]	Pd incorporated[b] (%)	Pd loading[b] (mmol g^{-1})	Pd content[b] (wt %)
1	**5a**	1:0.1	80	0.75	8.03
2	**5a**	1:0.05	96	0.45	4.81
3	**5a**	1:0.01	98	0.09	0.98
4	**5b**	1:0.1	81	0.77	8.14
5	**5b**	1:0.05	93	0.48	5.11
6	**5b**	1:0.01	96	0.09	0.96

[a]Mass ratio of **4a** or **4b** to Pd employed in the synthesis. [b]Determined via ICP-OES.

Representative TEM images of MNPs before (**4a** and **4b**) and after (**5a** and **5b**) Pd immobilization prepared from ethanol dispersions are shown in Figure 4. The average diameter of MNPs of **4a** was 8.9 ± 2.0 nm and that of **4b** was 9.6 ± 3.3 nm. These spherical particles are embedded in the polymer layer with some degree of nanoclustering (ca. 50−100 particles/cluster). In **5a** and **5b**, the spherical Pd nanoparticles are thoroughly dispersed on the MNP surface (4.9 ± 0.9 nm for Pd on **5a** and 3.7 ± 0.6 for Pd on **5b**). The magnified images of MNPs and Pd in the inset in Figure 4 exhibited the atomic lattice fringes owing to the crystalline nature of these particles. The interplanar spacing of 0.43 nm in **4a** and **4b** agreed with the (111) planes of Fe_3O_4 and that of 0.23 nm in **5a** and **5b** corresponded to the (110) planes of Pd nanoparticles.[54,55]

According to $M-H$ curves shown in Figure 5, saturation magnetization values (M_s) of **5a** and **5b** were 36.9 and 38.9

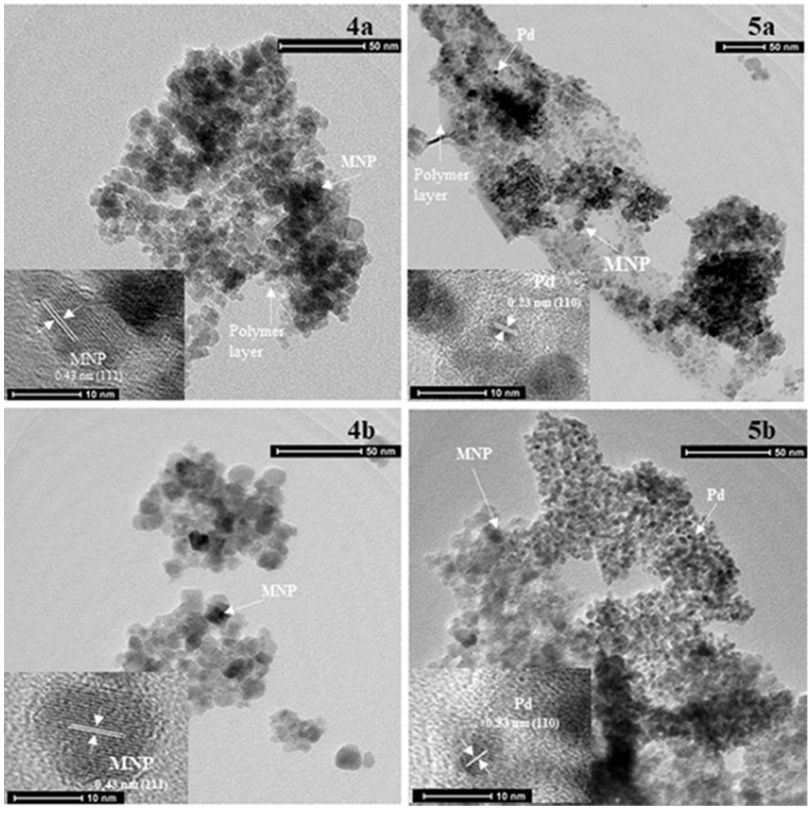

Figure 4. TEM images of MNPs before (**4a** and **4b**) and after (**5a**, entry 1, and **5b**, entry 4) Pd immobilization.

https://doi.org/10.1021/acsomega.3c00117
ACS Omega 2023, 8, 14531−14540

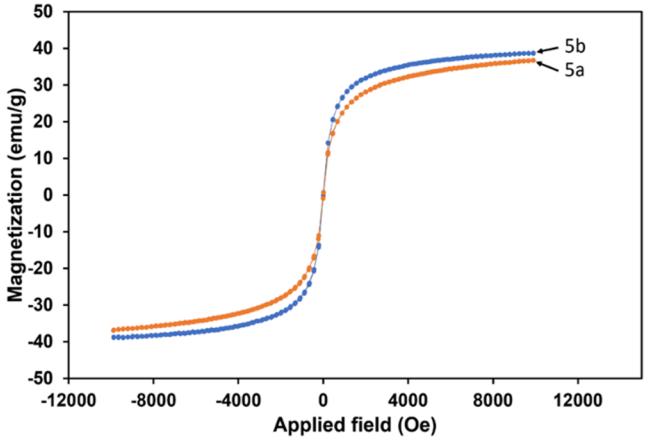

Figure 5. *M*−*H* curves of **5a** and **5b** showing their magnetic responsiveness properties.

emu/g, respectively, and consequently, both samples responded well to the external permanent magnet. They exhibited superparamagnetic behavior as indicated by the insignificant values of magnetic remanence (M_r) and coercitivity (H_c) (M_r values of **5a** and **5b** were 0.18 and 0.14 emu/g, and H_c values of **5a** and **5b** were 3.55 and 2.16 Oe, respectively). Interestingly, the M_s value of **5a** was slightly lower than that of **5b**, which was attributed to the higher percentage of nonmagnetic polymers in **5a**. This rationalization was confirmed by the results obtained from the TGA technique (see Supporting Information, Figure S2).

The catalytic activity of **5a** and **5b** in the hydrogenation of some alkenes and aromatic nitro compounds was subsequently investigated (Table 2). Sterically less hindered, strained, and activated alkenes were effectively hydrogenated to their corresponding alkanes within short reaction times to reach full conversion, achieving TOFs up to 750 h^{-1} (entries 1−4). In turn, chalcone, representing an electron-deficient alkene, required a considerably longer reaction time, but it could be also hydrogenated in quantitative yields (entry 5). Nitroarenes were also successfully hydrogenated to form anilines with full conversion (entries 6−8). The presence of deactivating (−Cl in entry 7) and activating ($-CH_3$ in entry 8) groups in the *para* position on the aromatic rings did not significantly affect the reaction rate. Comparing the activities of the catalysts with and without thermoresponsive PNIPAAm (**5b** vs **5a**), it was found that **5b** showed lower catalytic activities in all cases (entries 1−8). **5b** in the swollen form might somewhat inhibit the accessibility of the substrates to the catalysts, which is in good agreement with the results shown in Figure 3.

Recycling was studied at 25 and 45 °C to evaluate the catalytic activity of **5a** and **5b** after multiple uses at the temperatures below and above the LCST of the copolymer **5b** (Table S1 and Figure 6). The figure showing the hydrogenation step and the catalyst recovering step of this recycling is provided in Supporting Information (Figure S11). In all cases, catalyst recovery was readily achieved via applying an external magnet. The hydrogenation of 4-chlorostyrene in the presence of 1 mol % catalyst under ambient H_2 pressure in 2-propanol was used as a model reaction. For **5a**, full conversion was reached within 90−120 min irrespective of the reaction temperature (Figure 7A), being a consequence of the absence of thermoresponsive PNIPAAm in the structure. A slow decrease of catalytic activity was observed over 10 runs. Given the low Pd leaching (≤0.13% per run based on the initial palladium amount employed) from **5a** (Figure 8A), we attribute this activity loss to some alteration of the palladium nanoparticles (e.g., agglomeration) within the support.

Table 2. Hydrogenation of Olefins and Nitroarene Compounds Using 5b and 5a Catalysts in Hydrogenation at 25 °C and Stopped at Full Conversion[a]

Entry	Substrate	Product	Catalyst (mol%)	Time[b] (min)		TOF[c] (h^{-1})	
				5a	**5b**	**5a**	**5b**
1	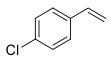	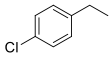	1.0	90	120	67	50
			0.1	150	180	400	333
2			1.0	112	100	54	60
			0.1	120	120	500	500
3			1.0	70	85	86	71
			0.1	80	80	750	750
4	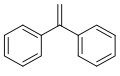	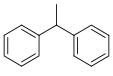	1.0	105	150	57	40
			0.1	180	160	333	375
5	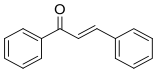	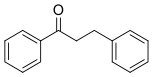	1.0	740	1080	8	6
6			1.0	260	340	23	18
7	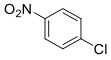	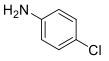	1.0	370	450	16	13
8	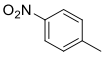		1.0	300	400	20	15

[a]Substrates (1 mmol) in isopropanol (10 mL) were hydrogenated by 0.1−1.0 mol % Pd catalyst at 25 °C under ambient H_2-pressure. [b]Determined by GC analysis using dodecane as an internal standard. [c]Mole of substrates transformed per mole catalyst per hour.

https://doi.org/10.1021/acsomega.3c00117
ACS Omega 2023, 8, 14531−14540

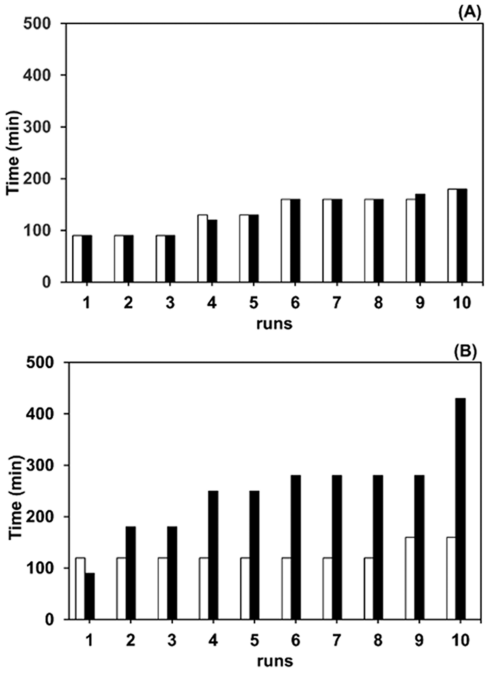

Figure 6. Recycling abilities of (A) **5a** and (B) **5b** catalysts for hydrogenation of 4-chlorostyrene at 25 °C (□) and 45 °C (■). The reactions were monitored by GC analysis and stopped at full conversion.

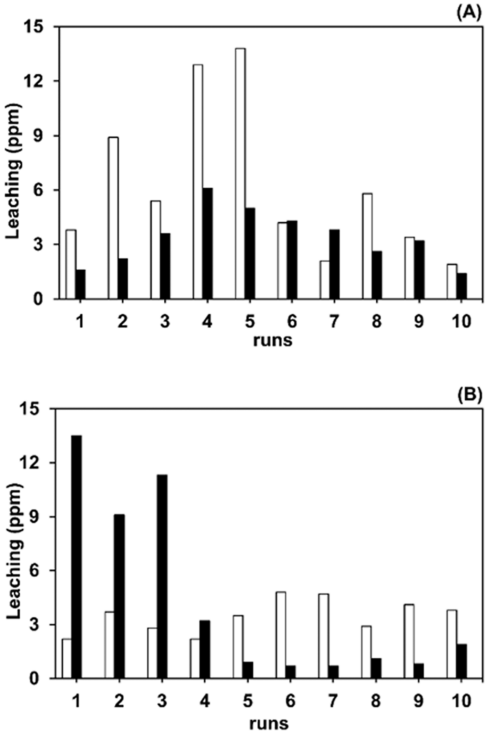

Figure 7. Leaching study of (A) **5a** and (B) **5b** catalysts for hydrogenation of 4-chlorostyrene at 25 °C (□) and 45 °C (■). These reactions were determined by ICP-OES analysis and stopped at full conversion.

For **5b**, a pronounced difference in the catalytic activity with respect to running the reactions below (25 °C) and above (45 °C) its LCST (37 °C) was observed (Figure 6B). The catalytic activity of **5b** at 25 °C seems to be slightly lower than that of

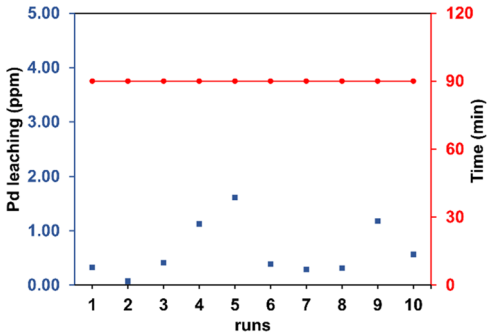

Figure 8. Recycling ability and leaching study of **5b** catalyst for hydrogenation of 4-chlorostyrene at 45 °C (90 min reaction time for completion of the reaction in all runs), followed by holding at 15 °C for 30 min after completing the reaction.

5a as indicated by the longer reaction time to reach a full conversion (120 min for **5b** and 90 min for **5a**). This was most likely due to the swelling of PNIPAAm units in **5b** below its LCST, which might somewhat inhibit the accessibility of the substrates to the catalyst for the hydrogenation. Notably, the catalytic activity remained constant during eight runs (120 min, 1st−8th runs, Figure 7B) with only a slight drop after that (160 min, 9th−10th runs, Figure 6B). The palladium nanoparticles might be well confined in swollen **5b**, being in good agreement with the low leaching (less than 5 ppm Pd leaching in each run, Figure 7B) observed. At 45 °C, the catalytic activity was initially slightly increased compared to 25 °C (1st run, Figure 7B), reflecting the collapse of the chains in the copolymer in **5b** at 45 °C (above its LCST), which might facilitate the accessibility of the starting materials to Pd catalyst for the hydrogenation. However, the catalytic activity of **5b**, being immediately isolated after each run by magnetic decantation, continuously dropped after repetitive uses, being reflected by a 4-fold longer reaction time to reach full conversion (1st run at ca. 100 min and 10th run at ca. 400 min). This was attributed to the agglomeration of palladium nanoparticles due to more degrees of freedom upon the shrinkage of the copolymer in **5b** at 45 °C (Figure 7).

To improve the process, the protocol for the recovery of **5b** was adjusted. Thus, the hydrogenation was performed at 45 °C to reach full conversion, and then the mixture was slowly stirred at 15 °C (below the LCST of the copolymer) for 30 min to allow for sufficient time for the polymer in **5b** to re-equilibrate to its original state, which might protect the palladium nanoparticles from agglomeration or oxidation, rather than immediately isolating the polymer by magnetic decantation. This way, the catalytic activity of **5b** could be maintained over 10 consecutive runs (90 min reaction time, Figure 8), indicating its improved reusability (Figure 9C). Additionally, the palladium leaching was now even lower (<1.6 ppm/run, total loss of Pd over 10 runs <0.1%) (Figure 8 and Table S2). Comparing the catalytic activity of **5b** during 10 runs using three different temperature protocols clearly shows the benefits of thermoresponsive units that allow access to the palladium catalyst above the LCST and also the importance of allowing the material to return to its original state upon cooling (Figure 9).

■ CONCLUSIONS

Thermoresponsive magnetic nanocatalysts embedded with Pd for the hydrogenation of olefins and nitro compounds were

https://doi.org/10.1021/acsomega.3c00117
ACS Omega 2023, 8, 14531−14540

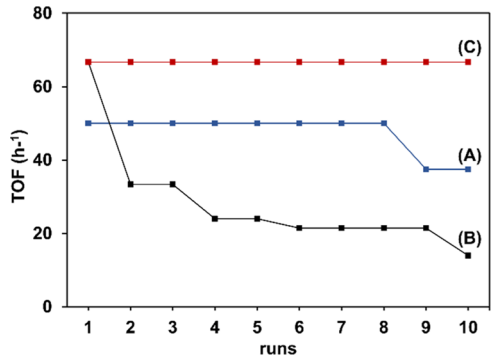

Figure 9. Recycling ability of **5b** catalyst (1 mol %) for hydrogenation of 4-chlorostyrene (1 mmol) in isopropanol (10 mL) under H_2 pressure at (A) 25 °C, (B) 45 °C, and (C) 45 °C, followed by holding at 15 °C for 30 min.

successfully synthesized. P(DEAEMA-*co*-NIPAAm)-coated MNP nanosupports were designed in such a way that they contain thermoresponsive moieties from PNIPAAm and coordinating parts to Pd from PDEAEMA units, while their magnetic core allows for easy and rapid recovery by magnetic separation. The catalytic activity of the nanocatalysts could be tuned by adjusting their temperature to below or above the LCST of the copolymer (37 °C) to obtain swollen/collapsed states, which greatly influences the hydrogen-substrate diffusion. The materials showed excellent reusability without a significant drop in catalytic activity for 10 consecutive runs, reflecting the efficient catalyst capture in the swollen polymers. This recyclable nanocatalyst with thermally tunable properties is therefore a promising platform for the hydrogenation of olefins and nitroarenes.

■ ASSOCIATED CONTENT

Supporting Information

The Supporting Information is available free of charge at https://pubs.acs.org/doi/10.1021/acsomega.3c00117.

^{1}H NMR spectrum; preparation of samples for ICP-OES analysis; GC data and chromatograms; TGA results; tables of recycling studies of **5b** and **5a** catalysts for hydrogenation; and recycling process (PDF)

■ AUTHOR INFORMATION

Corresponding Authors

Metha Rutnakornpituk − *Department of Chemistry and Center of Excellence in Biomaterials, Faculty of Science, Naresuan University, Phitsanulok 65000, Thailand;* orcid.org/0000-0002-0804-5233; Email: methar@nu.ac.th

Oliver Reiser − *Institute of Organic Chemistry, University of Regensburg, 93053 Regensburg, Germany;* orcid.org/0000-0003-1430-573X; Email: oliver.reiser@chemie.uni-regensburg.de

Authors

Sujittra Paenkaew − *Department of Chemistry and Center of Excellence in Biomaterials, Faculty of Science, Naresuan University, Phitsanulok 65000, Thailand; Institute of Organic Chemistry, University of Regensburg, 93053 Regensburg, Germany*

Usana Mahanitipong − *Department of Chemistry and Center of Excellence in Biomaterials, Faculty of Science, Naresuan University, Phitsanulok 65000, Thailand*

Complete contact information is available at: https://pubs.acs.org/10.1021/acsomega.3c00117

Funding

This study was funded by the National Research Council of Thailand (NRCT) and Naresuan University (N42A650330) and the Royal Golden Jubilee PhD Program (PhD/0210/2556).

Notes

The authors declare no competing financial interest.

■ ACKNOWLEDGMENTS

This project is funded by the National Research Council of Thailand (NRCT) and Naresuan University (N42A650330). SP thanks the Royal Golden Jubilee PhD Program (PhD/0210/2556) for the scholarship. The authors gratefully acknowledge the help of Andreas Hartl and Joachim Rewitzer from University of Regensburg for the ICP-OES measurements and Jakkrit Tummachote from Naresuan University for the PCS measurements.

■ ABBREVIATIONS

MNP, magnetic nanoparticle; NIPAAm, *N*-isopropylacrylamide; PDEAEMA, 2-(diethylamino)ethyl methacrylate; LCST, lower critical solution temperature; **4a**, poly(2-(diethylamino)-ethyl methacrylate)-coated MNP; **4b**, poly((2-(diethylamino)-ethyl methacrylate)-*co*-(*N*-isopropylacrylamide))-coated MNP; **5a**, palladium nanoparticles deposited onto poly(2-(diethylamino)ethyl methacrylate)-coated MNP; **5b**, palladium nanoparticles deposited onto poly((2-(diethylamino)ethyl methacrylate)-*co*-(*N*-isopropylacrylamide))-coated MNP

■ REFERENCES

(1) Ranga, S. Comparative analysis of homogeneous and heterogeneous catalysis. *Int. J. Eng. Sci. Res. Technol.* **2017**, *4*, 2394−3386.

(2) Baghbanian, S. M.; Farhang, M.; Vahdat, S. M.; Tajbakhsh, M. Hydrogenation of arenes, nitroarenes, and alkenes catalyzed by rhodium nanoparticles supported on natural nanozeolite clinoptilolite. *J. Mol. Catal. A* **2015**, *407*, 128−136.

(3) Chang, F.; Kim, H.; Lee, B.; Park, S.; Park, J. Highly efficient solvent-free catalytic hydrogenation of solid alkenes and nitro-aromatics using Pd nanoparticles entrapped in aluminum oxy-hydroxide. *Tetrahedron Lett.* **2010**, *51*, 4250−4252.

(4) Kwon, M. S.; Kim, N.; Park, C. M.; Lee, J.; Kang, K. Y.; Park, J. Palladium nanoparticles entrapped in aluminum hydroxide: Dual catalyst for alkene hydrogenation and aerobic alcohol oxidation. *Org. Lett.* **2005**, *7*, 1077−1079.

(5) Merckle, C.; Haubrich, S.; Blümel, J. Immobilized rhodium hydrogenation catalysts. *J. Organomet. Chem.* **2001**, *627*, 44−54.

(6) Roseblade, S. J.; Pfaltz, A. Iridium-catalyzed asymmetric hydrogenation of olefins. *Acc. Chem. Res.* **2007**, *40*, 1402−1411.

(7) Bergbreiter, D. E. Immobilized Catalysts, Solid Phases, Immobilization and Applications. In *Recent Progress in Polymeric Palladium Catalysts for Organic Synthesis*; Kirschning, A., Ed.; Springer-Verlag: Berlin, Chapter 3, 2004.

(8) Nasir Baig, R. B.; Varma, R. S. Magnetic carbon-supported palladium nanoparticles: An efficient and sustainable catalyst for hydrogenation reactions. *ACS Sustainable Chem. Eng.* **2014**, *2*, 2155−2158.

(9) Purohit, G.; Rawat, D. S.; Reiser, O. Palladium nanocatalysts encapsulated on porous silica @ magnetic carbon-coated cobalt

nanoparticles for sustainable hydrogenation of nitroarenes, alkenes and alkynes. *ChemCatChem* **2020**, *12*, 569−575.
(10) Llabrés i Xamena, F.; Abad, A.; Corma, A.; Garcia, H. MOFs as catalysts: Activity, reusability and shape-selectivity of a Pd-containing MOF. *J. Catal.* **2007**, *250*, 294−298.
(11) Baran, T.; Sargin, I.; Kaya, M.; Menteş, A.; Ceter, T. Design and application of sporopollenin microcapsule supported palladium catalyst: Remarkably high turnover frequency and reusability in catalysis of biaryls. *J. Colloid Interface Sci.* **2017**, *486*, 194−203.
(12) Kamari, Y.; Ghiaci, M. Incorporation of TiO_2 coating on a palladium heterogeneous nanocatalyst. A new method to improve reusability of a catalyst. *Catal. Commun.* **2016**, *84*, 16−20.
(13) Cattaneo, S.; Freakley, S. J.; Morgan, D. J.; Sankar, M.; Dimitratos, N.; Hutchings, G. J. Cinnamaldehyde hydrogenation using Au-Pd catalysts prepared by sol immobilisation. *Catal. Sci. Technol.* **2018**, *8*, 1677−1685.
(14) Puthiaraj, P.; Wha, S. A. Synthesis of copper nanoparticles supported on a microporous covalent triazine polymer: an efficient and reusable catalyst for *O*-arylation reaction. *Catal. Sci. Technol.* **2016**, *6*, 1701−1709.
(15) Kandasamy, G.; Sudame, A.; Luthra, T.; Saini, K.; Maity, D. Functionalized hydrophilic superparamagnetic iron oxide nanoparticles for magnetic fluid hyperthermia application in liver cancer treatment. *ACS Omega* **2018**, *3*, 3991−4005.
(16) Gawande, M. B.; Branco, P. S.; Varma, R. S. Nano-magnetite (Fe_3O_4) as a support for recyclable catalysts in the development of sustainable methodologies. *Chem. Soc. Rev.* **2013**, *42*, 3371−3393.
(17) Gawande, M. B.; Luque, R.; Zboril, R. The Rise of Magnetically Recyclable Nanocatalysts. *ChemCatChem* **2014**, *6*, 3312−3313.
(18) Hudson, R.; Feng, Y.; Varma, R. S.; Moores, A. Bare magnetic nanoparticles: sustainable synthesis and applications in catalytic organic transformations. *Green Chem.* **2014**, *16*, 4493−4505.
(19) Polshettiwar, V.; Luque, R.; Fihri, A.; Zhu, H.; Bouhrara, M.; Basset, J. M. Magnetically recoverable nanocatalysts. *Chem. Rev.* **2011**, *111*, 3036−3075.
(20) Kong, L.; Lu, X.; Bian, X.; Zhang, W.; Wang, C. Constructing carbon-coated Fe_3O_4 microspheres as antiacid and magnetic support for palladium nanoparticles for catalytic applications. *ACS Appl. Mater. Interfaces* **2011**, *3*, 35−42.
(21) Balaev, D.; Semenova, S. V.; Dubrovskiya, A. A.; Yakushkinc, S. S.; Kirillovc, V. L.; Martyanovc, O. N. Superparamagnetic blocking of an ensemble of magnetite nanoparticles upon interparticle interactions. *J. Magn. Magn. Mater.* **2017**, *440*, 199−202.
(22) Vikesland, P. J.; Rebodos, R. L.; Bottero, J. Y.; Rose, J.; Masion, A. Aggregation and sedimentation of magnetite nanoparticle clusters. *Environ. Sci.: Nano* **2016**, *3*, 567−577.
(23) Gomez, I. J.; Goodwin, W. B.; Sabo, D.; Zhang, Z. J.; Sandhage, K. H.; Meredith, J. C. Three-dimensional magnetite replicas of pollen particles with tailorable and predictable multimodal adhesion. *J. Mater. Chem. C* **2015**, *3*, 632−643.
(24) Dolatkhah, A.; Wilson, L. D. Magnetite/polymer brush nanocomposites with switchable uptake behavior toward methylene blue. *ACS Appl. Mater. Interfaces* **2016**, *8*, 5595−5607.
(25) Altan, C. L.; Gurten, B.; Sadza, R.; Yenigul, E.; Sommerdijk, N. A. J. M.; Bucak, S. Poly(acrylic acid)-directed synthesis of colloidally stable single domain magnetite nanoparticles via partial oxidation. *J. Magn. Magn. Mater.* **2016**, *416*, 366−372.
(26) Wang, D.; Park, C. M.; Masud, A.; Aich, N.; Su, C. Carboxymethylcellulose mediates the transport of carbon nanotube-magnetite nanohybrid aggregates in water-saturated porous media. *Environ. Sci. Technol.* **2017**, *51*, 12405−12415.
(27) Ma, Z.; Porosoff, M. D. Development of tandem catalysts for CO_2 hydrogenation to olefins. *ACS Catal.* **2019**, *9*, 2639−2656.
(28) Chang, J.; Guan, X.; Pan, S.; Jia, M.; Chen, Y.; Fana, H. Sulfonated poly(styrene-divinylbenzene-glycidyl methacrylate)-capsulated magnetite nanoparticles as a recyclable catalyst for one-step biodiesel production from high free fatty acid-containing feedstocks. *New J. Chem.* **2018**, *42*, 13074−13080.
(29) Ren, Y.; Li, H.; Yang, W.; Shi, D.; Wu, Q.; Zhao, Y.; Feng, C.; Liu, H.; Jiao, Q. Alkaline ionic liquids immobilized on protective copolymers coated magnetic nanoparticles: An efficient and magnetically recyclable catalyst for knoevenagel condensation. *Ind. Eng. Chem. Res.* **2019**, *58*, 2824−2834.
(30) Mai, B. T.; Fernandes, S.; Balakrishnan, P. B.; Pellegrino, T. Nanosystems based on magnetic nanoparticles and thermo- or pH-responsive polymers: an update and future perspectives. *Acc. Chem. Res.* **2018**, *51*, 999−1013.
(31) Yang, Y.; Xu, L.; Zhu, W.; Feng, L.; Lui, J.; Chen, Q.; Dong, Z.; Zhao, J.; Liu, Z.; Chen, M. One-pot synthesis of pH-responsive charge-switchable PEGylated nanoscale coordination polymers for improved cancer therapy. *Biomaterials* **2018**, *156*, 121−133.
(32) Du, L.; Xu, Z. Y.; Fan, C. J.; Xiang, G.; Yang, K. K.; Wang, Y. Z. A fascinating metallo-supramolecular polymer network with thermal/magnetic/light-responsive shape-memory effects anchored by Fe_3O_4 Nanoparticles. *Macromolecules* **2018**, *51*, 705−715.
(33) Rifaie-Graham, O.; Ulrich, S.; Galensowske, N. F. B.; Balog, S.; Chami, M.; Rentsch, D.; Hemmer, J. R.; Alaniz, J. R. D.; Boesel, L. F.; Bruns, N. Wavelength-selective light-responsive DASA-functionalized polymersome nanoreactors. *J. Am. Chem. Soc.* **2018**, *140*, 8027−8036.
(34) Dong, Y.; Jin, Y.; Wang, J.; Shu, J.; Zhang, M. Pd nanoparticles stabilized by a simple pH-sensitive P(acrylamide-co-acrylic acid) copolymer: A recyclable and highly active catalyst system in aqueous medium. *Chem. Eng. J.* **2017**, *324*, 303−312.
(35) Li, Y.; Zhu, L.; Wang, B.; Mao, Z.; Xu, H.; Zhong, Y.; Zhang, L.; Sui, X. Fabrication of thermoresponsive polymer-functionalized cellulose sponges: Flexible porous materials for stimuli-responsive catalytic systems. *ACS Appl. Mater. Interfaces* **2018**, *10*, 27831−27839.
(36) Zhou, H.; Chen, M.; Liu, Y.; Wu, S. Stimuli-responsive ruthenium-containing polymers. *Macromol. Rapid Commun.* **2018**, *39*, 1800372.
(37) Zhou, P.; Wang, S.; Tao, C.; Guo, X.; Hao, L.; Shao, Q.; Liu, L.; Wang, Y. P.; Chu, W.; Wang, B.; Luo, S. Z.; Guo, Z. PAA/alumina composites prepared with different molecular weight polymers and utilized as support for nickel- based catalyst. *Adv. Polym. Technol.* **2018**, *37*, 2325−2335.
(38) Dolatkhah, A.; Jani, P.; Wilson, L. D. Redox-responsive polymer template as an advanced multifunctional catalyst support for silver nanoparticles. *Langmuir* **2018**, *34*, 10560−10568.
(39) Chen, T.; Hua, L.; Zhang, S.; Xu, Z.; Zhou, L.; Wang, J. Synthesis of zinc(II) complex-containing thermo-responsive copolymer based on activated ester functionalization and its catalysis application. *Eur. Polym. J.* **2018**, *109*, 473−482.
(40) Kanidi, M.; Papagiannopoulos, A.; Skandalis, A.; Kandyla, M.; Pispas, S. Thin films of PS/PS-*b*-PNIPAM and PS/PNIPAM polymer blends with tunable wettability. *J. Polym. Sci., Part B: Polym. Phys.* **2019**, *57*, 670−679.
(41) Xin, B.; Hao, J. Reversibly switchable wettability. *Chem. Soc. Rev.* **2010**, *39*, 769−782.
(42) Sun, T.; Wang, G.; Feng, L.; Liu, B.; Ma, Y.; Jiang, L.; Zhu, D. Reversible switching between superhydrophilicity and superhydrophobicity. *Angew. Chem., Int. Ed.* **2004**, *43*, 357−360.
(43) Paenkaew, S.; Rutnakornpituk, M. Effect of alkyl chain lengths on the assemblies of magnetic nanoparticles coated with multifunctional thiolactone-containing copolymer. *J. Nanopart. Res.* **2018**, *20*, 193−205.
(44) Natalia, F.; Stoychev, G.; Puretskiy, N.; Leonid, I.; Dmitry, V. Porous thermo-responsive pNIPAM microgels. *Eur. Polym. J.* **2015**, *68*, 650−656.
(45) Li, L.; Zhao, H.; Wang, R. Tailorable synthesis of porous organic polymers decorating ultrafine palladium nanoparticles for hydrogenation of olefins. *ACS Catal.* **2015**, *5*, 948−955.
(46) Kainz, Q. M.; Linhardt, R.; Grass, R. N.; Vilé, G.; Ramírez, J. P.; Stark, W. J.; Reiser, O. Palladium nanoparticles supported on magnetic carbon-coated cobalt nanobeads: Highly active and recyclable catalysts for alkene hydrogenation. *Adv. Funct. Mater.* **2014**, *24*, 2020−2027.

https://doi.org/10.1021/acsomega.3c00117
ACS Omega 2023, 8, 14531−14540

(47) Linhardt, R.; Kainz, Q. M.; Grass, R. N.; Stark, W. J.; Reiser, O. Palladium nanoparticles supported on ionic liquid modified, magnetic nanobeads − recyclable, high-capacity catalysts for alkene hydrogenation. *RSC Adv.* **2014**, *4*, 8541−8549.
(48) Mondal, A.; Mondal, A.; Adhikary, B.; Mukherjee, D. K. Cobalt nanoparticles as reusable catalysts for reduction of 4-nitrophenol under mild conditions. *Bull. Mater. Sci.* **2017**, *40*, 321−328.
(49) Feng, A.; Zhan, C.; Yan, Q.; Liu, B.; Yuan, J. A CO_2- and temperature-switchable 'schizophrenic" block copolymer: from vesicles to micelles. *Chem. Commun.* **2014**, *50*, 8958−8961.
(50) Liu, L.; Wu, C.; Zhang, J.; Zhang, M.; Liu, Y.; Wang, X.; Fu, G. Controlled polymerization of 2-(diethylamino)ethyl methacrylate and its block copolymer with *N*-isopropylacrylamide by RAFT polymerization. *J. Polym. Sci., Part A: Polym. Chem.* **2008**, *46*, 3294−3305.
(51) Jain, K.; Vedarajan, R.; Watanabe, M.; Ishikiriyama, M.; Matsumi, N. Tunable LCST behavior of poly(*N*-isopropylacrylamide/ionic liquid) copolymers. *Polym. Chem.* **2015**, *6*, 6819−6825.
(52) Liu, R.; Fraylich, M.; Saunders, B. R. Thermoresponsive copolymers: from fundamental studies to applications. *Colloid Polym. Sci.* **2009**, *287*, 627−643.
(53) Hou, L.; Wu, P. LCST transition of PNIPAM-*b*-PVCL in water: cooperative aggregation of two distinct thermally responsive segments. *Soft Matter* **2014**, *10*, 3578−3586.
(54) Marquez, F.; Morant, C.; Sanz, J. M.; Elizalde, E. Post-synthesis alignment of chemically modified carbon nanotubes in magnetic fields. *J. Nanosci. Nanotechnol.* **2009**, *9*, 6127−6131.
(55) Yang, Y.; Duan, H.; Xia, S.; Lu, C. Construction of a thermoresponsive copolymer-stabilized Fe_3O_4@CD@PdNP hybrid and its application in catalytic reduction. *Polym. Chem.* **2020**, *11*, 1177−1187.

https://doi.org/10.1021/acsomega.3c00117
ACS Omega 2023, 8, 14531−14540